# Risk-Based Assessment of Seismic Repair Costs for Reinforced Concrete Bridges, Considering Competing Repair Strategies

**J. Valigura[1], A.B. Liel[2] and P. Sideris[3]**

**Abstract:**

This paper outlines a procedure to support selection of repair strategies for damaged structures after an earthquake. Under strong shaking, modern, code-compliant, bridges can sustain significant damage to their ductile members, and failure of sacrificial members. However, there are many choices of repair strategies, and no clear guidance on their selection. This paper proposes a seismic performance assessment framework to determine repair costs for reinforced concrete bridges, considering costs associated with both the initial repair and future expected seismic repairs (which are based on the performance of the repaired bridge). For initial repair, the paper considers several common column repair techniques, which are separately evaluated in terms of direct costs. For future expected repairs, the paper proposes a method to evaluate the effect of each of the repair strategies on a repaired bridge's post-repair future seismic performance to quantify the expected repair costs associated with each strategy over the remaining service life of the bridge. The

[1] Graduate Research Assistant and Ph.D. Candidate, Department of Civil, Environmental and Architectural Engineering, University of Colorado at Boulder, Boulder, CO, 80309, U.S.A. E-mail: Jakub.Valigura@colorado.edu

[2] Associate Professor, Department of Civil, Environmental and Architectural Engineering, University of Colorado at Boulder, Boulder, CO, 80309, U.S.A. (corresponding author). E-mail: Abbie.Liel@colorado.edu

[3] Assistant Professor, Zachry Department of Civil Engineering, Texas A&M University, College Station, TX, 77843, U.S.A. E-mail: Petros.Sideris@tamu.edu

procedure is demonstrated for two conventional concrete bridges, but can be applied to any concrete bridge or other bridges with some modifications in details. The results show the importance of considering post-repair performance in choice of repair strategies. Although the initial seismic repair costs of competing repair strategies are similar, some repaired bridges will incur higher repair costs in subsequent events. As a result, in cases where the repairs need to be performed early in the life of the bridge, the service life expected costs of strategies can differ by a factor of two.

**Keywords:** Concrete bridges; seismic response; column repair jackets; post-repair performance; repair costs.

## Introduction

Modern practice in seismic design of bridges aims to prevent collapse and loss of life for conventional bridges during strong earthquakes (Caltrans 2010). However, during such earthquakes, these bridges can experience extensive damage to their components. This damage can produce significant consequences for communities, due to repair costs and bridge closure. For example, following the 2014 Napa earthquake, Caltrans reported 21 damaged bridges, with total repair costs exceeding $2.75 million (Caltrans 2014). Once a bridge is damaged, it is inspected, the type of repairs is selected, and the repair is then designed and constructed (Veletzos et al. 2006). The selection of the repair technique is left to the expertise of the field engineer.

This study enhances the existing performance-based earthquake engineering (PBEE) framework for bridges, in terms of losses, i.e. repair costs, in several ways. In particular, it contributes a novel procedure that explicitly accounts for alternative repair methods in terms of initial direct costs. More importantly, the study subsequently shows how the post-repair performance of each repair strategy can be established and incorporated in the performance assessment framework. This approach considers that each strategy may have different implications in terms of future seismic response and, hence, damage and repair costs. To support the implementation of the framework, we propose a new set of damage states for modern reinforced concrete (RC) bridges that are consistent with damage assessment procedures used by field engineers in California, and tabulate and report associated repair costs. We further investigate and identify optimal intensity measures (IM) for 3D models of RC bridges.

In this paper, the proposed framework is applied to two prototype bridges representing modern conventional California highway overpass bridges. The bridges are subjected to incremental dynamic analysis (IDA) to simulate seismic demand, which serves as the input to damage

assessment and estimation of repair costs. Repairs are designed for different damage levels for abutments, superstructure and columns. For column repairs, we consider multiple, competing strategies. The bridges repaired with each of the techniques are then reanalyzed via IDA to examine the effect of the repairs on the post-repair performance, and to examine how the selected repair strategy impacts service-life economic impacts of repair costs. These results for the first time show general trends in repair costs and their distribution between different bridge components based on the bridge geometry, considering post-repair performance, and demonstrate the effect of each repair strategy on the initial stiffness, and strength and displacement capacity, and consequently on the repair cost outcomes. This study thus shows the necessity of including post-repair performance of the bridges in the selection of the repair methods.

## Background

### *State of Practice*

The design of conventional concrete bridges in seismic areas in the U.S. is governed by AASHTO (2011), while several states additionally have their own codes, such as Caltrans' (2013) Seismic Design Criteria for California. According to the philosophy of these documents, bridges are designed with ductile substructures (bridge piers/columns), sacrificial elements (shear keys, backwalls, bearings) and capacity-protected elements (superstructure, foundation, wingwall/stemwall). These design provisions intend to concentrate damage in parts of the bridge that are easily accessible for assessment and repairs after an earthquake. If a bridge is damaged in an earthquake, Caltrans has adopted a step-by-step guide (Veletzos et al. 2006) for determining damage and estimating the remaining capacity of bridge components. This method is based on visual inspection and the original performance of the bridge components, and aims to reduce variation among damage assessments from engineer to engineer.

The usual repair method for minor damage to RC columns is epoxy injection and patching of areas with spalled concrete. When columns experience more severe damage, RC jackets have been shown to successfully restore strength capacity (Lehman at al. 2001), and are often used (Caltrans, 2017b). Other repair options for damaged columns are steel or prestressed concrete jackets (Buckle et al. 2006), and, recently, fiber reinforced polymer (FRP) jackets (Vosooghi and Saiidi 2013; Yang et al. 2015). Experimental work has shown that all of these repairs can restore the flexural and shear strength of the columns to the as-built state, but the deformation capacity and stiffness may not be fully restored (Yang et al. 2015).

***Seismic Performance Assessment***

The PBEE methodology has been previously used to assess vulnerability of bridges in high seismic areas (Mackie et al. 2011; Yang et al. 2009; Kaviani et al. 2014). These studies showed that damage tends to concentrate in the abutments and columns. Mackie et al. (2011) also estimated repair costs and repair time under certain damage scenarios for some bridges. For example, for a 5-span RC relatively narrow bridge, abutment-related repairs represented the largest contribution to repair costs for major damage scenarios, and column repairs were the largest contributor in situations of minor damage. The PBEE methodology has also been applied to compare different bridge designs (e.g. Lee and Billington 2011; Jeong et al. 2008).

A number of studies have also specifically examined bridge retrofit and repair assessments. Herein, the term "*retrofit*" refers to changes that aim to enhance the performance of a seismically-deficient bridge prior to an earthquake, while the term "*repair*" defines procedures that aim to restore performance of bridges damaged during an earthquake. Padgett and DesRoches (2008) presented a methodology for developing fragility curves of retrofitted bridges, which was subsequently employed to compare retrofit methods. That work showed the effectiveness of

different retrofit measures to be a function of bridge type and damage state (Padgett and DesRoches 2009). Billah et al. (2013) analytically developed fragility curves for a multi-column bridge bent retrofitted by different methods. They concluded that engineered cementitious composite materials and carbon (C) FRP jackets were the most effective retrofitting techniques for reducing the fragility of that bent. Tapia and Padgett (2016) proposed a multi-objective optimization method to select structural retrofit and repair decisions for bridges to minimize initial economic costs. Illustrating the framework with a multi-span continuous steel girder bridge, the authors showed that 2.5% of all the combinations (most of which involved retrofitting steel bearings to elastomeric and installing seat extenders and shear keys) were near-optimal, i.e. resulting in lowest costs, but their optimization did not consider performance of the repaired bridges.

Jeon et al. (2016) used a "time-dependent" element to investigate differences in performance of damaged unrepaired and repaired (using CFRP and steel jackets) pre-1971 bridges. This "time-dependent" element activated repair members (i.e., jackets) for aftershock assessments, while maintaining the damage that was already sustained by the column. They found that bridges with columns repaired with steel jackets are slightly less damaged than bridges with columns repaired with CFRP jackets and that the unrepaired bridges performed worst. Deco et al. (2013) introduced a tool to perform a pre-event probabilistic comparison of the outcomes of different repair scenarios in terms of both direct and indirect costs. Their study defined a repair scenario as a set of repairs for all damage states (i.e. a scenario is a vector that consists of one repair for DS1, one repair for DS2, etc.). The study then calculates costs of the repair scenarios considering the likelihood of each damage state being experienced by the original bridge.

## Framework for seismic performance assessment of bridges considering multiple repair strategies

The present study builds on previous work to propose a framework for seismic performance assessment of bridges that explicitly considers multiple repair strategies and their post-repair performance. The proposed framework consists of separate PBEE assessment of the original and repaired bridges, with the assessment being performed for all repair strategies of interest. The outline of the framework is shown in Fig. 1.

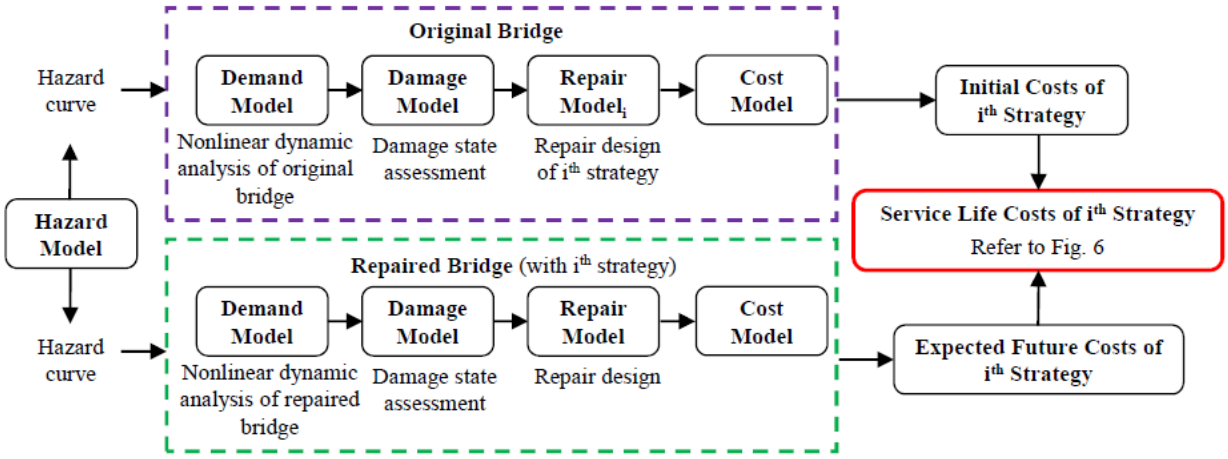


**Fig. 1.** Framework overview, showing the consideration of the i$^{th}$ repair strategy

The PBEE framework consists of four main components: a hazard model, a demand model, a damage model, and a decision model (Deierlein et al. 2003). The *hazard model* represents the likelihood that an intensity measure (IM) will exceed a certain level. The *demand model* relates IMs to engineering demand parameters (EDPs) using structural analysis. The *damage model* connects EDPs to damage states (DSs); DSs occur when an EDP exceeds a threshold defining the onset of that DS for a particular component. The *decision model* associates a DS with a decision variable (DV), which can be expressed as repair cost ($), repair time (days), or other metrics of

interest. Mackie et al. (2008) extended the decision model by separating it into a *repair model* and a *cost model* (shown in Fig. 1). The repair model determines quantities (Q) of materials, labor, and equipment that are needed to repair an element in a given DS. These quantities are economically evaluated in the cost model. The final result of a PBEE evaluation is the mean annual frequency of occurrence of the DV. This study focuses on a single DV, repair costs (sometimes referred to as "direct economic losses"), which are assessed for two prototype bridges. Our damage model considers damage to all major bridge components, and the effect of competing repair strategies for columns.

As highlighted in Fig. 1, the proposed framework then repeats the PBEE procedure to model and assess the bridge(s) with the one of the various repair strategies to quantify future seismic performance of the repaired bridge. Contrary to Jeon et al. (2016), we do not propose to use time-dependent elements or "back-to-back" dynamic assessment, but rather a separate analysis of the repaired structure under the same set of motions. This approach is more convenient for practicing engineers and reduces computational time, but some parts of the damage may not be fully captured by the model of the repaired bridge (see discussion below). The assessment of the repaired bridge is a novel contribution here (unlike Deco et al. (2013), Tapia and Padgett (2016) and others) because it incorporates post-repair performance, which can significantly affect the expected costs over the bridge's remaining service life, into the framework. Hence, this framework can be readily used to select the repair strategy with the lowest initial or projected service-life cost.

The PBEE methodology accounts for uncertainty in each of the models. The record-to-record variability in structural response is captured by simulating EDPs in multiple motions at a given IM level (FEMA 2012; Mackie et al. 2008); this uncertainty can be expanded to incorporate modeling uncertainty (*e.g.*, Liel et al. 2009; Padgett and DesRoches 2007). The uncertainty in DS observed

for a given EDP is expressed by establishing the onset threshold of a DS as a distribution (FEMA 2017; Mackie et al. 2008). The uncertainty in the repair model arises from uncertainties in quantities of material needed due to uncertainty in materials needed for construction or the extent of damage. Lastly, the variation in unit costs, which are used in the cost model, is due to competing material producers, seasonal demand of materials, distance to manufacturers, etc.

## Bridge design and simulation model

### *Selection and design of prototype bridges*

The proposed framework is applied to two bridges for which plans are available. These bridges are representative of post 2000 construction in California. "Representativeness" is evaluated with respect to the 2015 National Bridge Inventory (FHWA 2015), from which the authors identified trends in recent bridge construction in California, as discussed in Section S3.

Two bridges are selected for this study (more details in Table S3). Prototype bridge 1 (PB1) is model bridge No. 3a from Ketchum et al. (2004), while prototype bridge 2 (PB2) is the La Veta Avenue Overcrossing located in Orange, CA. The elevations and superstructure cross-sections of each bridge are shown in Fig. 2 and Fig. S2, respectively. PB1 is a 5-span post-tensioned concrete box girder superstructure bridge with four monolithic columns with a design PGA of 0.49 g. PB2 was designed with a design PGA of 0.40 g (ATC 1996) and constructed in 2001. This bridge has a 2-span RC box girder superstructure and a single pier with two columns. Where needed, the authors updated the design to satisfy recent design requirements (AASHTO 2011). The two bridges represent a range of geometric properties; PB1 has a relatively large number of columns with small superstructure cross-section and small abutments, while PB2 has small number of columns, but large superstructure cross-section and abutments. Both bridges are assumed to be located in Orange, CA.

The authors designed abutments for both bridges based on the current state of practice and specifications (Caltrans 1994a, 1994b, 2013), with design details provided in Section S3.

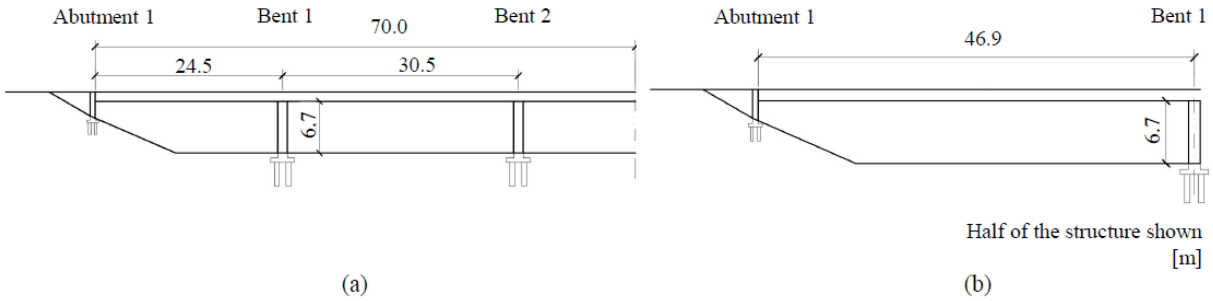


**Fig. 2.** Bridge elevations: (a) PB1 and (b) PB2

***Nonlinear simulation models***

The bridges are modeled in three dimensions in OpenSEES (McKenna et al. 2000) as a spine model. This approach represents the bridge superstructure and columns with beam-column (line) elements connected along the central axis of the members. Mass is lumped at multiple nodal locations along each span to capture dynamic behavior. Geometric nonlinearities are considered via the corotational transformation. Stiffness-proportional damping of 2% is assigned to the last-committed and initial stiffness (in a ratio of 3:2), an approach which has been observed to provide good predictions of residual drifts without significantly altering maximum drifts (Jeong et al. 2008; Tazarv and Saiidi 2013).

A schematic of the bent model for PB2 is shown in Fig. 3 (the model for PB1 is similar). The columns are modeled using a single gradient inelastic (GI) flexibility-based beam-column element (Sideris and Salehi 2016; Salehi and Sideris 2017) for the clear height of the column and rigid links to connect the top of the column with the centroid of the superstructure. Each GI column element is comprised of several fiber sections over its length. These sections consist of fibers for the confined core, fibers for the unconfined concrete, and fibers for the longitudinal steel

reinforcement (using a computationally-efficient material model that can capture both bar fracture and buckling). More information on the nonlinear model and the steel model developed by the authors is provided in Section S4.

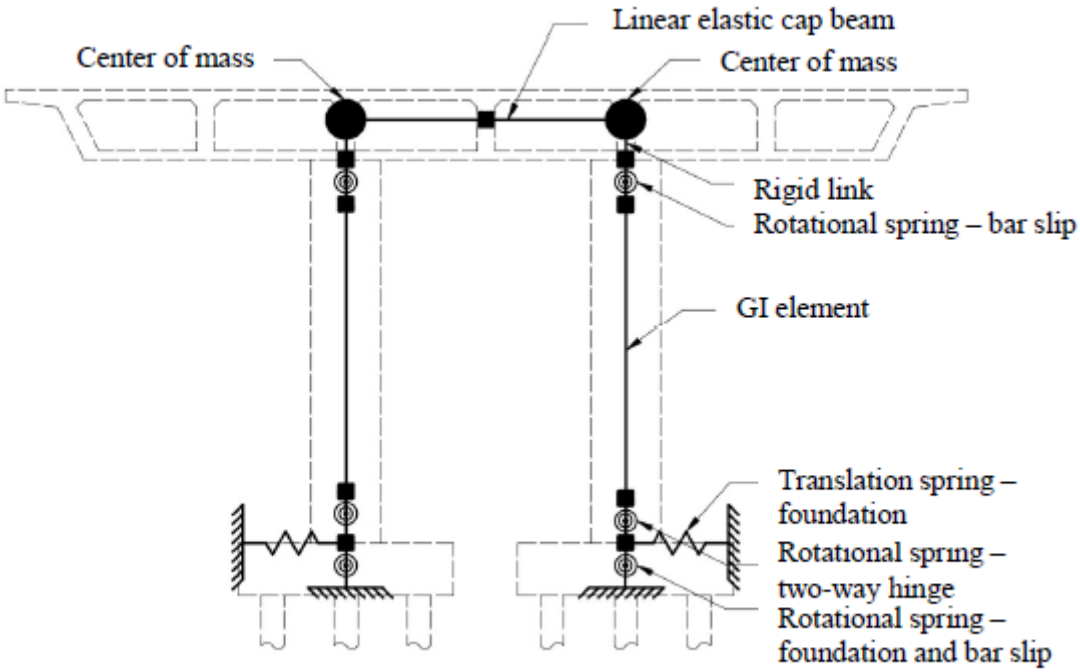


**Fig. 3.** *OpenSEES* model of PB2 bridge bent, showing configuration of foundation springs, GI elements, and masses

The soil-structure interaction for both bridges is modeled using translational and rotational linear springs that consider the foundation design (see Section S3). The superstructure is modeled using linear-elastic elements. The abutments are modeled using combinations of nonlinear zero-length springs (Fig. S6). Additional rotational springs at the bottom and top of each column are considered to simulate bar slip. More information on modeling can be found in Section S4.

In addition, the bridges are re-modeled with each of the repair strategies. For the sake of clarity of the procedure, this modeling approach is described in a separate section below.

## Demand model

To develop a demand model, the 3D nonlinear models of the bridges are analyzed using IDA. In IDA, the model of a structure is subjected to seismic excitation represented by a suite of ground motions, with each ground motion incrementally scaled up until collapse (Vamvatsikos and Cornell 2002). In this study, the model of each bridge is subjected to a set of 39 far-field ground motions (Haselton and Deierlein 2008). The analysis uses both horizontal components of each motion.

We adopt an IM based on the average spectral acceleration, $Sa_{avg}$ (Eads et al. 2015), defined in Equation 1:

$$Sa_{avg,T\ or\ L}(0.8T_{1,T\ ot\ L}, \ldots, 1.5T_{1,T\ or\ L}) = \left(\prod_{i=1}^{N} Sa(a_i T_{1,T\ or\ L})\right)^{1/N} \quad (1)$$

$Sa_{avg}$ is the geometric mean of $Sa$ computed over the given period range. We consider $Sa_{avg}$ in the range of $0.8T_1$ to $1.5T_1$ in the transverse ($T$) and longitudinal ($L$) directions, with $N$ being the number of 0.01 s increments in the period range; each period considered is denoted $a_i T_1$. We use the arithmetic mean of $Sa_{avg}$ in the two orthogonal directions, denoted $\overline{Sa_{avg}}$,:

$$\overline{Sa_{avg}} = (Sa_{avg,T} + Sa_{avg,L})/2 \quad (2)$$

$Sa_{avg}$ avoids problems with the elastic $Sa(T_1)$ IM because it quantifies the spectral shape of each motion in proximity to its fundamental period, and captures the effect of period elongation as the structure enters the nonlinear range. The analysis conducted to select the IM is described in Section S1.

The damage model considers damage to all major bridge components. For each component, a set of DSs is defined, which may be defined based on several different EDPs. After dynamic analysis of the structure is performed, the joint distribution of EDPs for each IM level is quantified.

Subsequently, Monte Carlo Simulation (MCS) is utilized, and many (appropriately correlated) EDP realizations per IM level are generated, as described in Section S2. The randomly generated EDPs are compared with the randomly generated onset of each DS (described below) to determine the extent of the damage and design the repair for each component of the bridge.

**Damage states**

DSs are stablished for each component from field and experimental observations, as well as engineering judgment. Likewise, the EDP used to define the DSs are based on experimental results and engineering judgment. Regardless of the associated EDP, the onset of a DS is assumed to follow a lognormal distribution. The procedure to calculate the values of median and logarithmic standard deviation follows recommendations from FEMA P-58 (FEMA 2012). The onset of the DS is treated as uncertain in the MCS.

***Column damage states***

Several researchers have tested and defined DSs for ductile columns (Lehman et al. 2001; Vosooghi and Saiidi 2013; Yang et al. 2015). The DSs are usually described qualitatively ("extensive spalling", etc.). In this study, the qualitative DS descriptions provided by Vosooghi and Saiidi (2010) are adopted and associated with six quantitative damage states, as reported in Table 1. DS6 is subdivided into DS 6a and 6b; these DS can be triggered by rebar buckling or fractured, respectively, but their consequence is the same, and they can occur separately or together. The choice of EDP associated with each DS is taken from the Caltrans damage inspection guideline (Veletzos et al. 2006). The DS threshold medians and logarithmic standard deviations are calculated from data sets or equations that are presented in the relevant references.

**Table 1.** Column damage states

| DS | Qualitative description | EDP | Median threshold | Logarithmic (ln) std. dev. of threshold | Reference |
|---|---|---|---|---|---|
| DS1 | Flexural cracks | Cover tensile strain at the ends of the column | 0.008 | 0.40 | Goodnight et al. (2016) |
| DS2 | First spalling | Cover compressive strain at the ends of the column | 0.00381 | 0.25 | Mattock et al. (1961) |
| DS3 | Extensive spalling | Cover compressive strain at distance of 0.1D* from the column ends | 0.00381 | 0.25 | Mattock et al. (1961) |
| DS4 | Visible transverse and/or longitudinal rebar | Cover compressive strain at distance of 0.5D* from the column ends | 0.00381 | 0.25 | Mattock et al. (1961) |
| DS5 | Start of core failure | Core strain at the ends of the column | ** Calculated | 0.34 | Mander et al. (1988); Saatcioglu and Razvi (1992) |
| DS6a | Bar buckling | Compressive strain in rebar at the ends of the column | ** Calculated | 0.41 | Mander et al. (1994); Bayrak and Sheikh (2001); Bae et al. (2005); Dhakal and Maekawa (2002) |
| DS6b | Bar fracture | Tensile strain in rebar at the ends of the column | 0.146 | 0.17 | Bournonville et al. (2004) |

* D refers to column diameter

** Calculated from cross-section geometry and properties of transverse and longitudinal reinforcement for each cross-section

***Abutment damage states***

Damage to abutments designed to the latest Caltrans specifications is concentrated in bearings, in shear keys in the transverse direction, and in backwall and backfill in the longitudinal direction. All of these are referred as "sacrificial elements". Details about the DS definitions are provided in Table S4. Other abutment components, such as stemwall, wingwall or foundation, are capacity protected and, hence, unlikely to get damaged.

Steel-reinforced elastomeric bearings have three different failure modes based on their slenderness (Konstantinidis et al. 2008): slipping, i.e. failure due to friction force between the bearing and concrete being exceeded, "roll-over" and "roll-off" (see Section S5). For the selected

bridges, the authors determined that slipping is the limiting failure mode and occurs at median shear strains of 250% (PB1) and 240% (PB2) (Caltrans 1994a). Failure due to slipping is the only DS defined for the bearings.

In the transverse direction, the shear keys are designed to shear off before the capacity of wingwall or abutment foundation is reached (Bozorgzadeh et al. 2006). The shear key DSs are based on our engineering judgment, as a percentage of the shear key displacement capacity (refer to Section S5 and Fig. S5a).

The backwall DSs are based on experimental work (Bozorgzadeh 2007). That study observed that the peak resisting force of backwall and backfill occurs at 1.5% drift ratio of backwall (measured as maximum lateral displacement of the top of the backwall over the height of the backwall), and the residual strength around 4.5% of drift ratio (refer to Section S5 and Fig. S5b).

***Superstructure damage states***

Although the superstructure is a capacity-protected element and is expected to remain essentially elastic, some minor damage may occur. First, surface damage may occur due to impact between the superstructure and shear keys and/or backwall, when the gaps close. This damage is already captured in the DS (and repairs) of abutment elements. The second type of damage is associated with strains in superstructure due to longitudinal loads and moments, and consequent crack formation. Thus, two simultaneous DS associated with flexural cracks and compressive microcracks are defined in Table S5.

***Global damage states***

The column DSs in Table 1 do not explicitly consider residual drift. At a certain level of residual drift, it is too difficult to reset the structure to its original position (Kawashima and Unjoh 1997). This paper follows Lee and Billington (2011), who proposed that columns with residual

drift larger than 1% may require replacement, and that all columns with residual drift of 1.5% and larger require replacement. A linear function was adopted as a fragility curve between these limits. If the residual drift DS occurs together with one of DS1-6, the repair solution for the residual drift DS governs.

Collapse of the bridges is defined here as instability of the bridge and/or unseating of the superstructure in the longitudinal direction. Unseating occurs when the longitudinal displacement of the superstructure exceeds the seat width of the abutments; seat widths are reported in Section S5. After the superstructure unseats, collapse occurs from failure of the girders due to extensive negative moments above the bent closest to the abutment. Collapse due to instability occurs when P-delta effects cause the displacement of the superstructure to continue to increase after the ground motion ends.

## Repair strategies and costs

Despite Caltrans sponsoring several projects to evaluate CFRP and other repair methods (*e.g.*, Saini and Saiidi (2013) or Vosooghi and Saiidi (2013)), there is a lack of standards or guides to inform design of repairs for bridges after an earthquake. However, Caltrans does provide *retrofit* specifications for steel and FRP jackets (Caltrans 2008, 2011). In this paper, repairs are designed based on recent research on repair methods and these retrofit specifications.

### *Column repairs*

Repair methods for the columns are summarized in Table 2. The repairs for DS1 and 2 are nonstructural and are performed for durability reasons. For DS3 through 5, we consider four jacketing techniques, considering jackets made of RC, steel (Caltrans 2011), CFRP (Vosooghi and Saiidi 2013), and prestressed (post-tensioned) concrete (Buckle et al. 2006). If DS6 occurs, the column is replaced (Lehman et al. 2001).

**Table 2.** Column repair methods

| DS | Repair | Reference |
|---|---|---|
| DS1 | Epoxy injections | Lehman at al. (2001), Goodnight et al. (2016) |
| DS2 | Patching | Lehman at al. (2001), Goodnight et al. (2016) |
| DS3 | Concrete replacement, Construction of jacket (RC, Steel, CFRP, Prestress) | Caltrans (2011, 2013); Vosooghi and Saiidi (2013); Buckle et al. (2006) |
| DS4 | | |
| DS5 | | |
| DS6 (a,b) | Column replacement | Lehman et al. (2001) |

The jackets designed for DS3 through 5, illustrated in Fig. 4, are intended to restore shear strength that was lost from yielding of the transverse reinforcement and from cracking of concrete, and to restore confinement needed to provide flexural strength and deformation capacity. In order to compare the performance of different jackets, all jackets are designed to the minimum dimensions and confinement requirements of retrofit standards. In the case of RC jackets, a target confinement pressure is implicitly considered by requirements for the minimum transverse reinforcement ratio (Caltrans 2013). However, this may lead to the confining pressure provided by the RC jacket to be lower than for the rest of the repair jackets. For the other repair jackets, the minimum target confinement pressure is 2 MPa (300 psi) as recommended in retrofit and repair contexts (Buckle et al. 2006; Caltrans 2008, 2011; Vosooghi and Saiidi 2013). The height of the jackets is equal to the plastic hinge region height (as per Caltrans retrofit guidelines). Vosooghi and Saiidi (2013) provide estimates of losses in shear strength capacity of the original cross-section based on the DS the column experienced, which informs the shear strength design of all the repair strategies.

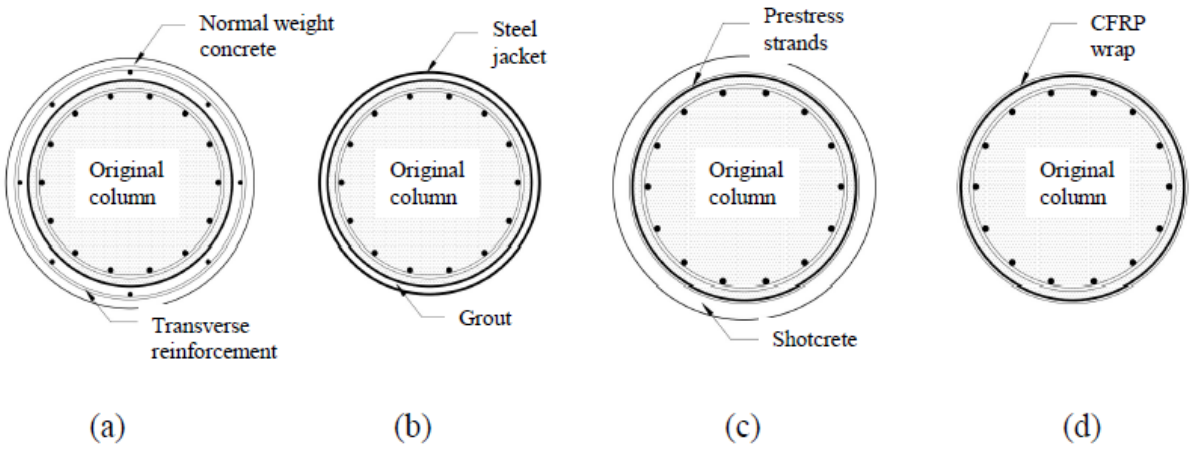


334

335 **Fig. 4.** Cross-sections of columns repaired with: (a) RC, (b) steel, (c) prestressed, and (d) CFRP jackets

336 ***Abutment repairs***

337 The repair of abutment involves repairs of bearings, shear keys, and backwall (including joint
338 seals and backfill). These repairs are summarized in Table S6. The bearings have only one DS
339 (failure), the occurrence of which implies that bearings need to be replaced. For the shear keys, the
340 repair for DS1 consists only of cleaning and patching of the superstructure and shear key surface
341 damaged by pounding. DS2 requires further repair of the surface area, re-centering of the shear
342 key, and patching/grouting of the shear plane. DS3 and 4 require replacement of the shear key.
343 The vertical reinforcement of the new shear key is doweled into the existing stemwall to ensure
344 sufficient displacement capacity.

345 In the longitudinal direction, damage to the abutment occurs in the joint seals (or joint seal
346 assembly), backwall and backfill. The repair for DS1 requires replacing the joint seal. During DS2,
347 the repair involves additional cleaning and patching concrete chipped by pounding between
348 superstructure and backwall. The repair of DS3 consists of excavation and new backfill of half of
349 the slip zone (Fig. S7), and patching of the backwall. For DS4, the entire backfill is excavated and
350 filled, and the backwall and approach slab are replaced.

Other studies looking at bridge repair costs (*e.g.*, Mackie et al. (2011)) explicitly reported costs due to bearing repairs, shear keys repairs, etc. This study, however, adds these element repair costs together and reports them as abutment repair costs.

***Superstructure repairs***

The repair of DS1 consists of applying a sealing resin on 30% of the superstructure surface. DS2 is treated with epoxy injections applied on 30% of the surface, summarized in Table S7. This surface percentage is based on estimates of others (Mackie et al. 2011).

***Repair cost estimation***

The unit costs of all repair materials and processes are estimated from data of all bids awarded by Caltrans between the first quarter of 2014 and the first quarter of 2017 (Caltrans 2017). The unit costs (in 2017 dollars) for repairs include material cost, as well as labor and equipment cost that are associated with placing that material.

The consequence functions employed here are trilinear models of unit cost versus quantity, as recommended by FEMA P-58 (FEMA 2012), with the parameters determined using the segmented regression method (Ryan and Porth 2007), based on the collected data. For example, the authors found that concrete was used for approach slabs in 38 projects during this time period. The authors collected the quantity and unit cost from each of these projects and used the data points to create consequence function, as shown in Fig. 5. For all the unit costs, the parameters are provided in Table S8.

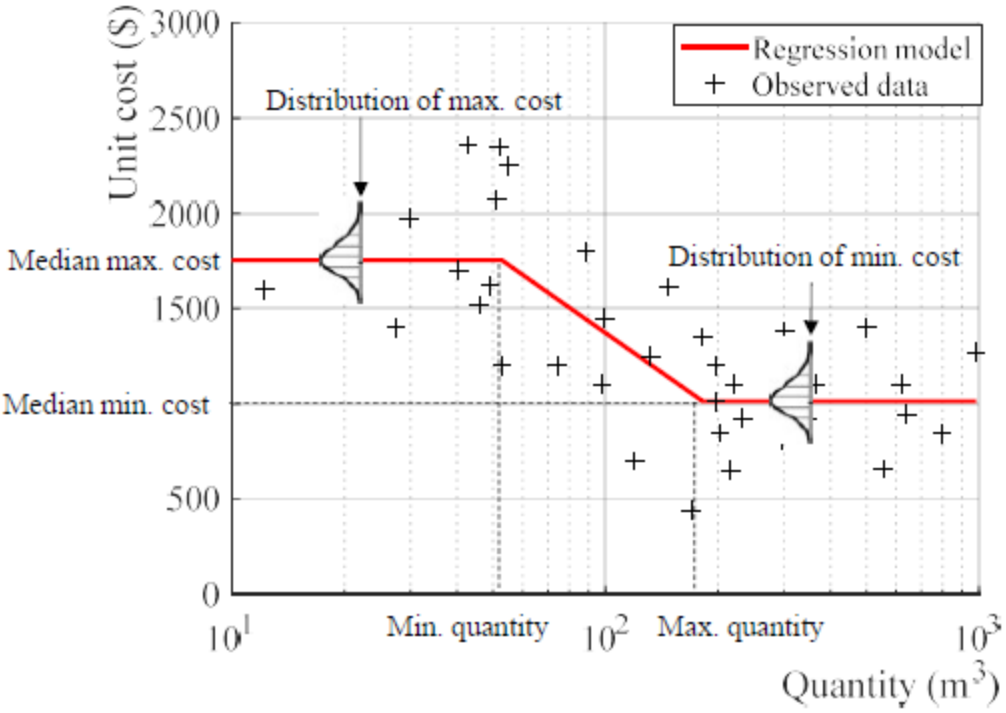


**Fig. 5.** Consequence function model developed by the authors for unit costs for concrete used for approach slabs, showing regression superimposed on observed data (collected by authors).

## Incorporating Seismic Performance of Repaired Bridges

### *Modeling of repaired bridges*

The post-repair performance of each alternative column repair strategy is investigated by creating nonlinear simulation models of the repaired bridges and subjecting them to the seismic performance assessment. The model of the repaired bridges assumes that the repair jackets are constructed around all column plastic hinges; this is a reasonable assumption given the high correlations between plastic hinging at the top and bottom of a given column and among different columns. The columns are then modeled using separate GI elements for the repaired and unrepaired parts of the column, as shown in Fig. S8.

382 The material constitutive models in the repaired part of the column are adjusted to account for
383 both previous damage and the change in confinement due to the repair jackets. Specifically, the
384 stiffness of longitudinal steel (*i.e.*, existing rebar) model is reduced using recommendations by
385 Vosooghi and Saiidi (2013) to account for previous yielding. The concrete material confined by
386 RC, steel, and prestressed jackets follows Mander et al. (1988)'s model, while the concrete
387 material confined by CFRP jacket follows an average of the models proposed by Jiang and Teng
388 (2007) and Spoelstra and Monti (1999), as illustrated in Fig. S4. The unrepaired part of the column
389 assumes the same material properties as the original column, as damage in those parts is assumed
390 to be insignificant. This approach differs from Jeon et al. (2016), who uses back-to-back analysis,
391 and hence can capture the damage in middle part of the column, but the effects are not expected to
392 be substantial.
393 For both bridges, the design of the each repair jacket for DS3 through 5 is governed by
394 minimum thickness or confinement requirements (Buckle et al. 2006; Caltrans 2008, 2011, 2013)
395 and thus, the dimensions and properties of each jacket type for all three DS are the same. As a
396 result, only four simulation models (one per repair strategy) are analyzed for post-repair
397 performance. Each of these models represent the bridge as repaired with one of the repair jacket
398 strategies after any of DS3-5; the steel material model stiffness for longitudinal rebar
399 conservatively assumes occurrence of DS5. If in fact the bridge experienced DS3 or DS4, this
400 assumption will slightly underestimate the stiffness (<2% difference) of the bridge.
401 ***Damage states and repair actions for repaired columns***
402 The columns repaired with RC and prestressed jackets are assumed to have the same DS set as
403 defined for RC columns in Table 1. However, in the case of steel and CFRP jackets, a new set of
404 DSs for each repair strategy is needed, detailed in Table 3. Experimental tests on columns

retrofitted or repaired with steel and CFRP jackets showed that only minimal damage is observed until extensive yielding or buckling of the steel jacket (Priestley et al. 1994), or rupture of the CFRP jacket (Vosooghi and Saiidi 2013). This damage requires replacement of the jackets in either case. The minimum thickness of steel jacket prevents the buckling of the jacket and hence it is not considered here. It is assumed that the entire column will be replaced if rebar buckling or fracture occurs. We are not concerned about the rebar buckling DS in the case of steel jackets, because even the yielded jacket can provide enough confinement to restrict the longitudinal rebar from buckling.

For the sake of clarity of comparisons, we assume that if the repaired columns need extensive repairs in subsequent seismic events, they would be repaired with the same type of repair jackets.

**Table 3.** Damage states of columns repaired with steel and CFRP jackets

| DS | Qualitative description | EDP | Median of threshold | Log. (ln) std. dev. of threshold | Reference |
|---|---|---|---|---|---|
| Steel jacket | | | | | |
| DS1 | Extensive yielding of the jacket | Compressive and tensile strain in the jacket at the ends of the column | 0.05 | 0.4 | Priestley et al., (1994) |
| DS2 | Bar fracture | Tensile strain in rebar at the ends of the column | 0.15 | 0.17 | Bournonville et al. (2004) |
| CFRP jacket | | | | | |
| DS1 | Fracture of the jacket | Compressive strain in the jacket at the ends of the column | * Calculated | | Vosooghi and Saiidi (2013) |
| DS2a | Bar buckling | Compressive strain in rebar at the ends of the column | ** Calculated | 0.41 | Mander et al. (1994); Bayrak and Sheikh (2001); Bae et al. (2005); Dhakal and Maekawa (2002) |
| DS2b | Bar fracture | Tensile strain in rebar at the ends of the column | 0.15 | 0.17 | Bournonville et al. (2004) |

* Calculated from the mechanical properties of the CFRP and number of layers in the jacket

** Calculated from geometry and properties of transverse and longitudinal reinforcement for each cross-section

***Post-repair performance assessment***

To compare the impacts of repair decisions and post-repair performance over the service life of the bridge for different repair strategies, we propose decision curves that quantify the present value of expected repair costs over the service life of the bridge (75 years). In this framework (shown in Fig. 6), the present value of the total repair cost over the service life of the bridge ($C_T$) comes from two sources: the costs of repairing the bridge during an initial earthquake ($C_I$), and the costs of repairing the repaired bridge due to future seismic hazard over the remaining service life ($C_E$) after the initial earthquake. The initial earthquake shaking is assumed to be strong enough that it warrants column repair by the jacket repairs being compared here (*i.e.*, putting columns in DS3 - 5). In essence, we choose to condition our decision curves on an initially damaging event, because it brings to light differences in post-repair behavior, while providing a "level playing ground" for investigation of the repair strategies; however, the assessment is not strictly hazard consistent.

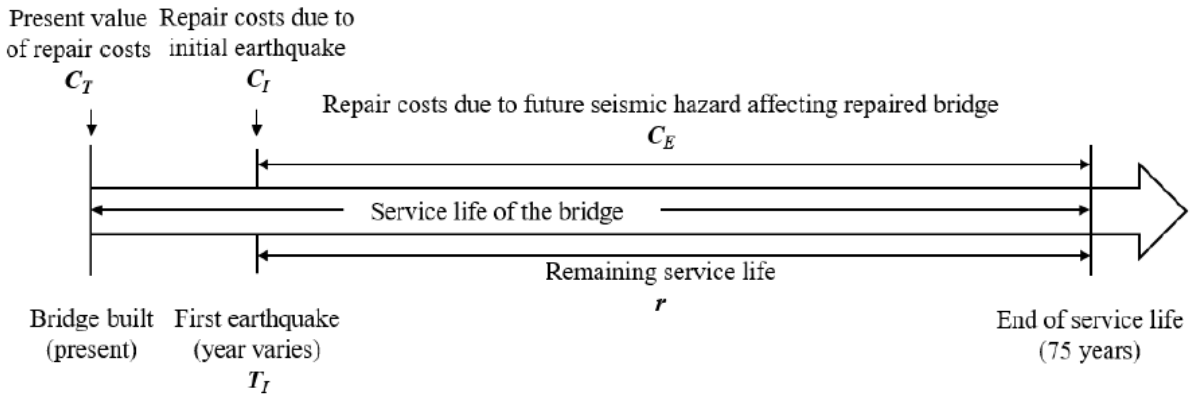


**Fig. 6.** Outline of method to calculate decision curves proposed for comparing service life impact of different repair strategies

To create the decision curve for a given repair strategy, we first assume and vary the year when the first earthquake ($T_I$), causing initial damage, strikes. The remaining service life ($r$) then depends

438 on $T_I$. The total repair costs ($C_T$) then consist of summation of repair costs at the time of the initial
439 earthquake ($C_I$), and the expected repair costs over the remaining service life if future
440 earthquake(s) occurs, causing damage to the already-repaired bridge ($C_E$). To obtain $C_I$, a
441 distribution of total repair costs for the original bridge associated with column DSs 3-5 is created.
442 This lognormal distribution comes from the repair cost assessment for the original bridge. To
443 determine $C_E$, first, each of the repaired bridge models is subjected to IDA and the repair costs are
444 assessed using the same procedure employed for the original bridge. Then, annualized losses
445 ($AL_{CE}$) for each repaired bridge are calculated by convolving the repair costs curve and hazard
446 curve (FEMA 2012). The hazard curve is treated deterministically (Section S8 provides details on
447 construction of hazard curve in terms of $\overline{\mathrm{Sa}_{\mathrm{avg}}}$), while the cost curve is treated probabilistically
448 (see Section S9). The value of $C_E$ at time $T_I$, considering the remaining service life of the bridge
449 and accounting for the real interest rate ($k$), assumed to be 3% (Zerbe and Falit-Baiamonte 2001),
450 is determined according to Equation 3:

$$C_E = \frac{1 - e^{-kr}}{k} AL_{CE} \tag{3}$$

451 A realization of the present value (year 0) of total repair costs over the remaining service life is
452 calculated according to Equation 4:

$$C_T = (C_I + C_E)(1 + k)^{-T_I} \tag{4}$$

453 The framework employs MCS to generate 5000 realizations of $C_I$ and $C_E$ for different values
454 of $T_1$. The hazard assessment is Poissionian or time-independent (meaning the initial earthquake
455 does not affect the shaking intensity of future events). For simplicity, this study does not consider
456 deterioration with time.
457

## Seismic performance assessments with competing repair strategies

### *Expected repair costs for original bridges*

The expected repair costs for columns for the original bridges are shown in Fig. 7 as a function of the IM level normalized by the design value (designated as $\overline{DSa_{avg}}$) for each bridge. This normalization is carried out in order to compare results for bridges with different design values. Repair costs are normalized by costs of new construction for each bridge (Caltrans 2015; Ketchum et al. 2004) (see Section S7) and converted to 2017 dollars.

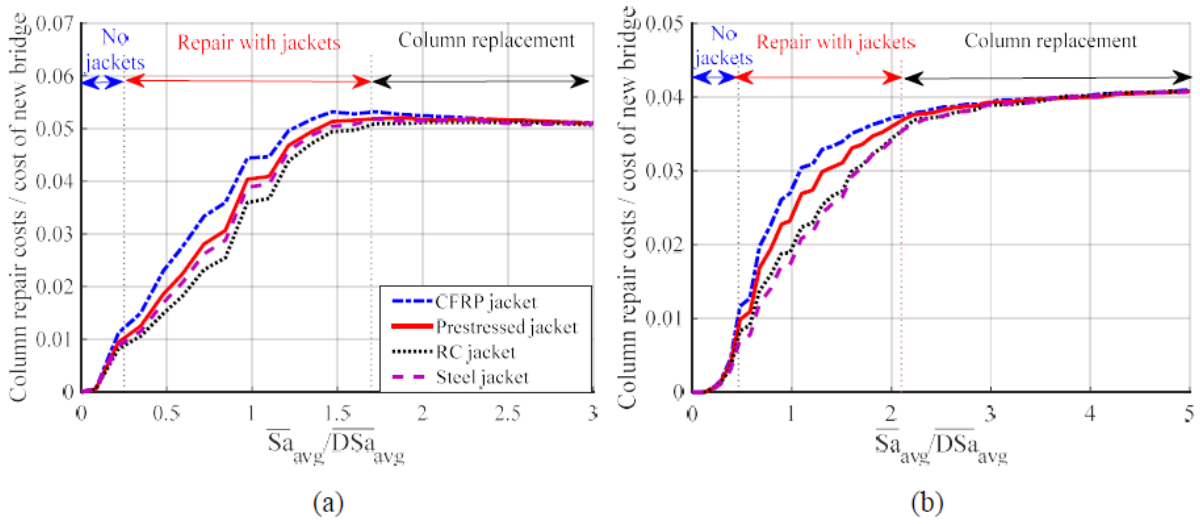


**Fig. 7.** Expected column repair costs, normalized by the total replacement cost of the bridge, for: (a) PB1 and (b) PB2

Three distinct regions of response can be identified:

1) A low intensity shaking region: here, the differences in expected repair costs among different repair strategies are minimal. Damage to columns is not extensive, and repairs consist mostly of epoxy injections and patching.
2) A medium intensity shaking region: the damage in this region is significant enough to require jacketing. In this region, the repair costs associated with the CFRP jackets are the largest

because of the larger unit costs of the CFRP material and its application. The most cost-efficient strategies are RC jackets for PB1 and steel jackets for PB2. The design of the steel jackets is governed by the minimum thickness of the jacket (10 mm = 0.4 in) based on Caltrans (2011)'s retrofit design aid. However, this thickness is greater than that needed to satisfy the confinement and shear demands. Hence, when the diameter of the column increases (from PB1 to PB2), the jacket material increases only by the column surface area that needs to be covered (proportional to square of the column diameter). Conversely, in the case of the RC jacket, the design is governed by the transverse reinforcement requirements. Hence, when the diameter increases, the transverse reinforcement amount is increased both by the column surface area that needs to be covered as well as by higher amount of reinforcement needed to confine the larger diameter (proportional to cube of the column diameter). As a result, the steel jacket is more cost-effective for the larger diameter columns (as in PB2).

3) A high intensity shaking region: here, the damage to columns is extensive, due to buckling or fracture of the longitudinal rebar, or large residual displacements. As a result, the differences in expected repair costs among different repair strategies are again minimal, because the most likely outcome is that columns are replaced.

Although there are differences associated with the column repair strategies (Fig. 7), these are not significant when the repair costs of the entire bridge are considered. Thus, for simplicity, the total repair costs in Fig. 8 are shown only for the bridges repaired with CFRP and steel jackets.

Fig. 8 shows contributions of repair costs from different elements for the steel jacket case, which are very similar to the other repaired strategies. The results show that the goal of non-collapse even during large seismic events is satisfied, with very small probability of collapse during the design earthquake. The costs associated with superstructure repair are insignificant for

both bridges, as expected based on the superstructure being a capacity protected element.

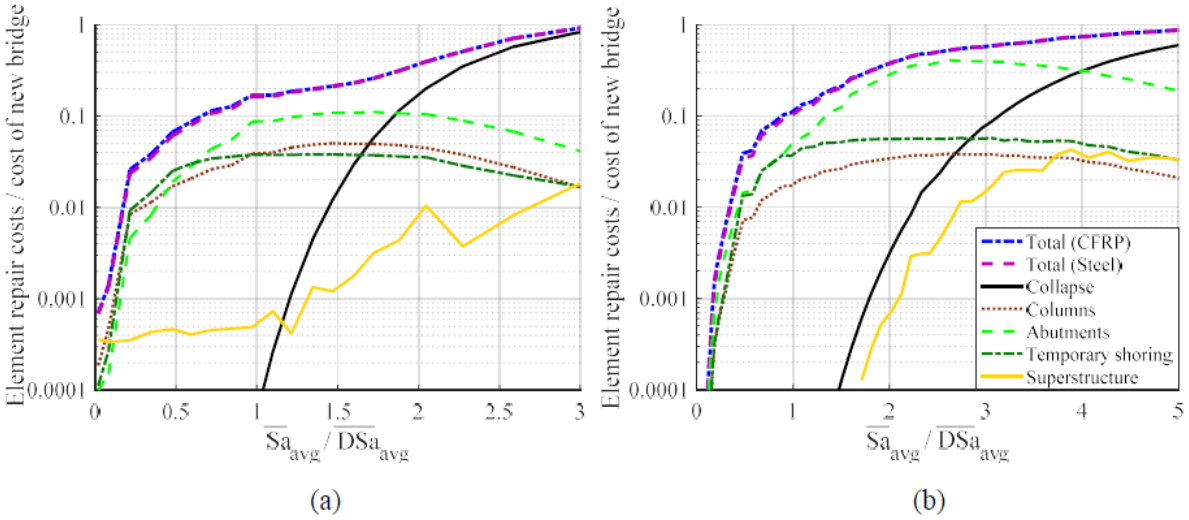


**Fig. 8.** Expected bridge repair costs, normalized by the total replacement cost of the bridge, and their breakdown for: (a) PB1 and (b) PB2

For PB1, the column repair costs have a higher contribution than abutment repair costs (totaling shear key, bearing, and backwall costs) at low IM values (up to about 0.5 times the design value), but at greater shaking intensities the abutment repairs have the highest contribution. At low IM values, the abutment components are "protected" by the gap between the superstructure and shear keys / backwalls. For PB2, the abutment repair costs have the highest contribution even at low IM levels. This important contribution occurs due to the larger size of the abutment, which increases the amount of material needed to repair the abutment components relative to PB1. In general, abutment repair costs will be most critical for bridges with a few long spans (due to increase in the height of the superstructure to limit the deflections under gravity loads) and with wide superstructures (e.g., PB2). The contribution of column repair costs tends to increase with the number of spans/columns.

513 ***Post-repair performance***

514 Results of pushover analysis of the original (undamaged) and repaired bridges, illustrated in
515 Fig. 9, offer the first insight into the post-repair behavior of the repaired bridges. In the case of
516 PB1, all repair strategies, except RC jackets, provide greater displacement capacity and flexural
517 strength than the original columns (Fig. 9a). The CFRP, steel and prestressed jackets are designed
518 explicitly to 2MPa (300 psi) confining pressure, while in the design of original bridge and RC
519 jacket repair, the confining pressure is implicitly considered in the minimum shear reinforcement
520 (Caltrans 2013). For these two cases, the actual confining pressure may be lower, explaining the
521 lower deformation capacity. Conversely, the minimum thickness of the steel jacket required by
522 Caltrans (2011) more than provides sufficient confinement and shear strength, resulting in
523 significant increases in the deformation capacity and ultimate strength of the column. The analysis
524 indicates that the initial stiffness of bridges repaired with RC and prestressed jackets is slightly
525 increased due to the increased dimensions of the jackets relative to the original column (and
526 because these models neglect the effects of previous cracking in the non-repaired part of the
527 column).

528 Fig. 9b shows, in the case of PB2, that only the steel jacket enhances the displacement capacity
529 of the columns. The steel jacket is effective because the minimum thickness requirement still
530 governs, but by smaller margin than in the case of PB1. The prestressed and CFRP jackets manage
531 to essentially restore the flexural and displacement capacities of the original bridge. The RC jacket
532 restores neither the displacement nor the moment capacity. When examining initial stiffness of
533 PB2, unlike PB1, none of the repair strategies manages to restore it to the original value (Fig. 9b).
534 The thickness of the repair jackets remains the same regardless of the diameter of the original
535 column and, hence, for columns with larger diameter (e.g., PB2), the jackets will add relatively

less stiffness; eventually, as the diameter of the column increases, the jackets cannot restore the stiffness. Large scale tests have confirmed that RC jackets can restore stiffness for tested diameters (e.g. Lehman et al. (2001)), but these columns are not as large as those considered here. CFRP jackets have been shown to not fully restore stiffness even for the small diameters (Vosooghi and Saiidi 2013).

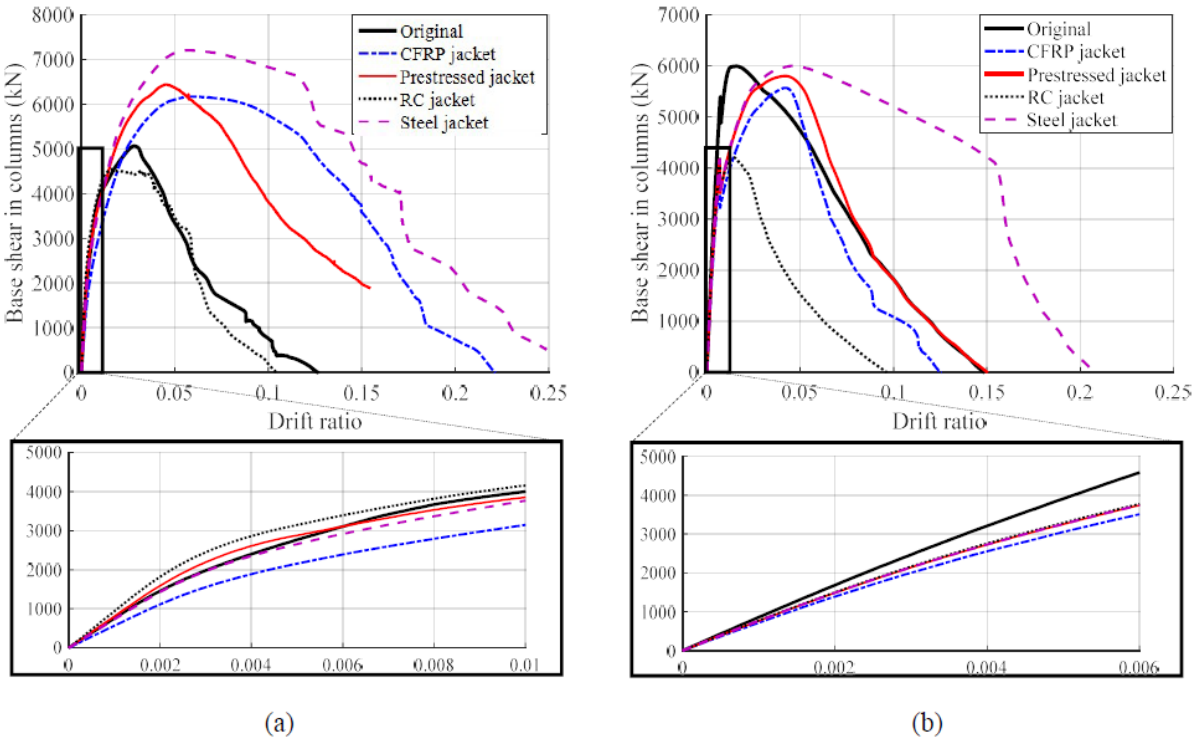


**Fig. 9.** Pushover results for: (a) PB1 and (b) PB2

The performance of each of the repair methods can be also examined by quantifying the seismic repair costs of the repaired bridge as a function of IM. These results, shown in Fig. 10, confirm the pushover analysis conclusions. The initial stiffness and element repair cost contribution govern the costs at lower IMs. Damage of bridge elements is related to the displacements of the superstructure and, hence, more flexible bridges experience, in general, higher damage and repair costs. At higher IM levels, the performance depends primarily on the

549 likelihood of collapse, which is inversely correlated with deformation capacity. Hence, bridges
550 with higher displacement capacities have lower expected repair costs in this range of response.
551 When a bridge does not collapse, the repair costs are always relatively low (because the most
552 expensive component, the superstructure, does not need to be replaced).

553 In the case of PB1, the steel jacketed bridge has lower expected repair costs compared to the
554 rest of the jacketing strategies, as shown in Fig. 10a. Steel jackets are followed by CFRP,
555 prestressed, and RC jackets at high IM levels, confirming the dependence on deformation capacity
556 in this regime. The CFRP-jacketed bridge has the lowest initial stiffness, which is exhibited with
557 highest repair costs at low IMs, due to abutment damage. On the other hand, the repair costs at low
558 IMs for RC and prestressed jacketed bridges, which are stiffer, come from minor damage to
559 columns due to cracking and spalling. The original bridge has relatively high repair costs, because
560 it is not as stiff.

561 Fig. 10b shows that, for PB2, the steel jacket has generally lower repair costs than the rest of
562 the repair methods, followed by prestressed, CFRP, and RC jackets. Due to similar deformation
563 capacities of the prestressed, CFRP and original bridges, the repair cost curves are similar in the
564 high IM level region. The original bridge has the best performance for lower IM levels, due to its
565 stiffness. The CFRP repaired bridge again shows the highest repair costs at low IMs.

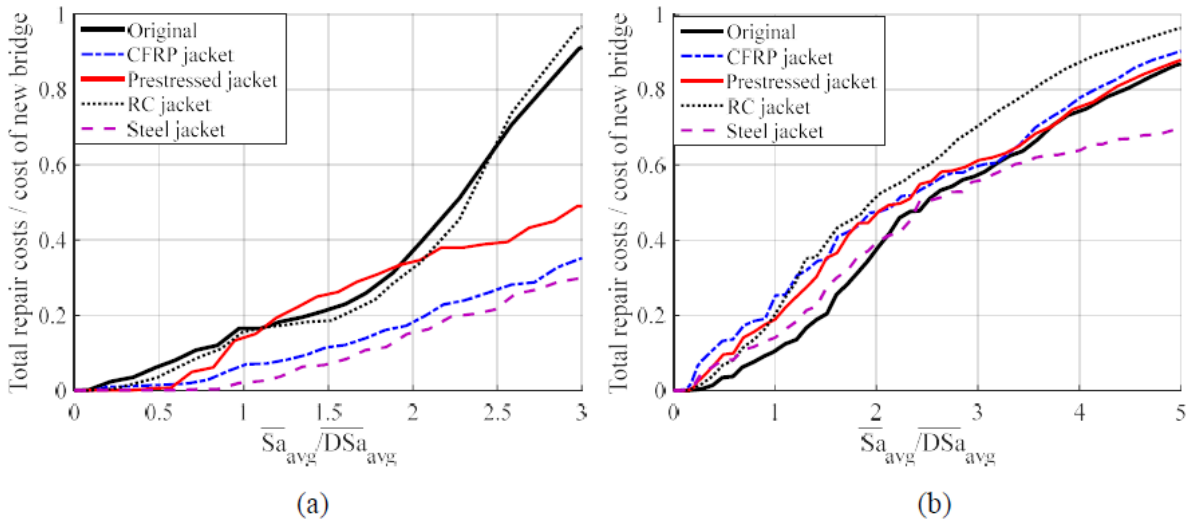


**Fig. 10.** Expected repair cost curves for repaired bridge alternatives for: (a) PB1 and (b) PB2

***Service-life repair costs***

To facilitate comparison of repair strategies, decision curves based on expected repair costs over the entire service life of the bridge are calculated, as illustrated in Fig. 6, with results plotted in Fig. 11.

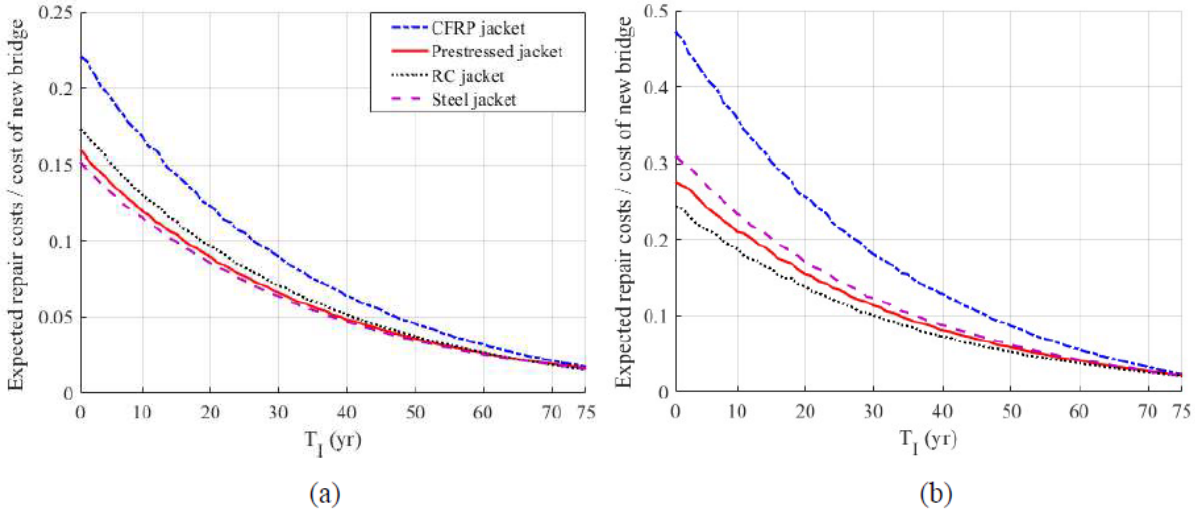


**Fig. 11.** Present value of expected repair costs over the service life considering the occurrence of a strong earthquake causing initial damage at different times in the service life for: (a) PB1, and (b) PB2

Results above show that, for the selected bridges, the costs of each of the repair strategies are relatively similar after the first earthquake (Fig. 8). Hence, differences in expected repair costs over the service life of the bridge are driven by the post-repair performance, i.e. the performance of the repaired bridge in subsequent earthquake(s). For the selected site, the future repair costs are governed by the low intensity events (which have high frequency of occurrence). As a result, the repair strategies with worse performance at the low IMs have higher service life repair costs compared to strategies with better performance at low IMs. The lowest service life repair costs are predicted for the steel jacket repairs for PB1, and RC jackets for PB2.

Most importantly, this study documents the implications of accounting for the post-repair performance of the bridge. If repair strategies are selected solely on the basis of the repair costs after the first earthquake (Fig. 8), RC and steel jackets would be the selected strategy for PB1 and PB2, respectively. When the post-repair performance is considered, the most desirable strategy swaps between the two bridges. In the post-repair context, initial stiffness plays a great role, and its effect is amplified by the dimensions of abutments. The strategy that most affects stiffness depends on the material and size of jackets relative to columns.

## Conclusions

This paper presents a comprehensive seismic performance assessment framework for RC bridges that accounts for competing repair strategies and their seismic performance. The framework has two parts. In the first part, it compares the initial costs of each repair strategy. However, the main novelty comes in the second part of the framework, where it provides a procedure for explicitly accounting for differences in seismic performance of the repaired bridges. As a result, projected repair costs that consist of the initial costs and the future seismic repair costs of the repaired bridge are determined. This step is of particular importance because previous

598 experimental studies at the component level have shown that the competing repair strategies do
599 not have the same performance.

600 In addition, we offer some detailed methodological improvements to facilitate this framework.
601 To minimize the uncertainty in the results, the study introduces an optimized intensity measure for
602 3D nonlinear models of reinforced concrete bridges. This intensity measure is selected based on
603 its low dispersion and high correlation with demand parameters of several major bridge
604 components. Furthermore, to allow for direct comparison between damage observed in the field
605 and during numerical simulations, this study presents definition of damage states for all bridge
606 components that are consistent with recommendations for post-earthquake visual assessment of
607 real structures, but are also readily available from results of numerical simulations. A database of
608 repair costs is also developed and tabulated for use by other researchers.

609 The proposed framework is then applied to two RC bridges. The results demonstrate that the
610 seismic performance of the bridges repaired with these strategies can be quite different. Hence, the
611 expected repair costs over the service life of the bridge are driven by the post-repair performance.
612 Indeed, in the cases shown here, a decision based on the repair costs after the first earthquake does
613 not minimize estimated service-life repair costs. As a result, this analysis demonstrates the
614 importance of selecting repair strategies considering the future seismic performance of the bridge.

615 In addition, although the selected bridges do not characterize an entire class of bridges, some
616 general conclusions and recommendations can be drawn from the results. The examples show that
617 the difference in repair costs in a given earthquake associated with competing column repair
618 strategies is relatively small (about 2% of the costs of a new bridge). As a result of this low
619 difference in cost, there is potential for the post-repair performance to play a significant role in
620 repair strategy selection process. RC and steel jackets are shown to have the lowest initial repair

costs, with steel jackets being more cost effective for columns with larger diameters. In addition, the studies show that abutment repair costs have a greater contribution to total repair costs than column repair costs even in the least favorable configuration (large number of columns and small dimensions of the abutment), and the contribution increases with the size of the superstructure (and consequently of abutment elements). This observation is important because it helps to select repair strategies that reduce projected future repair costs. Repairs that can better restore initial stiffness will often result in lower future repair costs, because the higher stiffness postpones the abutment damage. Lastly, especially for small diameter columns, the design of the column repair jackets is often driven by minimum dimensions requirements. This can lead to a significant improvement in performance. As the column diameter enlarges, other factors start to govern the design and the degree of overdesign, and, with it, the relative improvement in performance decreases.

## Acknowledgments

This research is funded by the National Science Foundation (NSF) under Award No. CMMI 1538585/1748031. Any opinion, findings, and conclusions or recommendations expressed in this article are those of the authors and do not necessarily reflect the views of NSF. The authors would also like to acknowledge the contributions and suggestions of Mohammad Salehi (Graduate Student, Texas A&M University).

## Supplemental data

Figs. S1–S9 are available online in the ASCE Library (ascelibrary.org).

Tables S1–S8 are available online in the ASCE Library (ascelibrary.org).

Sections S1–S9 are available online in the ASCE Library (ascelibrary.org).

## References


AASHTO. (2011). *AASHTO Guide Specifications for LRFD Seismic Bridge Design (2nd Edition) with 2012, 2014 and 2015 Interim Revisions*. Washington, DC.

ATC (Applied Technology Council). (1996). "Improved Seismic Design Criteria for California Bridges: Provisional Recommendations." *ATC-32*, Redwood City, CA.

Bae, S., Mieses, A. M., and Bayrak, O. (2005). "Inelastic Buckling of Reinforcing Bars." *Journal of Structural Engineering*, *131*(2), 314–321., 10.1061/(ASCE)0733-9445(2005)131:2(314).

Bayrak, O., and Sheikh, S. A. (2001). "Plastic Hinge Analysis." *Journal of Structural Engineering*, *127*(9), 1092–1100, 10.1061/(ASCE)0733-9445(2001)127:9(1092).

Billah, A. H. M. M., Alam, M. S., and Bhuiyan, M. A. R. (2013). "Fragility Analysis of Retrofitted Multicolumn Bridge Bent subjected to Near-Fault and Far-Filed Ground Motion." *Journal of Bridge Engineering*, *18*(10), 992–1004, 10.1061/(ASCE)BE.1943-5592.0000452.

Bournonville, M., Dahnke, J., and Darwin, D. (2004). "Statistical Analysis of the Mechanical Properties and Weight of Reinforcing Bars." *SL Report 04-1*. Structural Engineering and Materials Laboratory, The University of Kansas.

Bozorgzadeh, A. (2007). "Effect of Structure Backfill on Stiffness and Capacity of Bridge Abutments." *PhD Thesis*. University of California, San Diego.

Bozorgzadeh, A., Megally, S., Restrepo, J. I., and Ashford, S. A. (2006). "Capacity Evaluation of Exterior Sacrificial Shear Keys of Bridge Abutments." *Journal of Bridge Engineering*, *11*(5), 555–565, 10.1061/(ASCE)1084-0702(2006)11:5(555)

Buckle, I. G., Friedland, I., Mander, J., Martin, G., Nutt, R., and Power, M. (2006). "Seismic Retrofitting Manual for Highway Structures: Part 1 - Bridges." *Report No. FHWA-HRT-*

667 *06-032*. Federal Highway Administration.
668 Caltrans. (1994a). *Memo to Designers 7-1,* California Department of Transportation, Sacramento,
669 CA.
670 Caltrans. (1994b). *Memo to Designers 7-10,* California Department of Transportation,
671 Sacramento, CA.
672 Caltrans. (2008). *Bridge Design Aids 14-3: Fiber Reinforced Polymer (FRP) Composites Column*
673 *Casing Systems*, California Department of Transportation, Sacramento, CA.
674 Caltrans. (2010). *Memo to Designers 20-1*, California Department of Transportation, Sacramento,
675 CA.
676 Caltrans. (2011). *Bridge Design Aids 14-2: Steel Column Casing Design and Details,* California
677 Department of Transportation, Sacramento, CA.
678 Caltrans. (2013). *Caltrans Seismic Design Criteria Version 1.7,* California Department of
679 Transportation, Sacramento, CA.
680 Caltrans. (2014). *Bridge Investigation Team Report for the August 24, 2014 South Napa*
681 *Earthquake*, California Department of Transportation, Sacramento, CA.
682 Caltrans. (2015). *Construction Statistics 2015*. California Department of Transportation,
683 Sacramento, CA.
684 Caltrans. (2017a). "Contract Cost Data." <http://sv08data.dot.ca.gov/contractcost/index.php>
685 (September 14, 2017)
686 Caltrans. (2017b). "Project Bucket Search." <http://www.dot.ca.gov/des/oe/project-bucket-
687 output.php> (September 14, 2017)
688 Deco, A., Bocchini, P., & Frangopol, D. M. (2013). A Probabilistic Approach for the Prediction
689 of Seismic Resilience of Bridges. *Earthquake Engineering and Structural Dynamics*,

690 *42*(10), 1469–1487.
691 Deierlein, G. G., Krawinkler, H., and Cornell, C. A. (2003). “A Framework for Performance-Based
692 Earthquake Engineering.” *Proc., Pacific Conference on Earthquake Engineering*, New
693 Zealand Society for Earthquake Engineering, Christchurch, New Zealand, 1-8.
694 Dhakal, R. P., and Maekawa, K. (2002). “Reinforcement Stability and Fracture of Cover Concrete
695 in Reinforced Concrete Members.” *Journal of Structural Engineering*, *128*(10), 1253–
696 1262, 10.1061/(ASCE)0733-9445(2002)128:10(1253).
697 FEMA. (2012). “Seismic Performance Assessment of Buildings Volume 1 - Methodology.” *FEMA*
698 *P-58-1*, Federal Emergency Management Agency, Washington, DC.
699 FEMA. (2017). “Hazus - MH 2.1: Technical Manual.” Federal Emergency Management Agency,
700 Washington, DC.
701 FHWA. (2015). “National Bridge Inventory.” <https://www.fhwa.dot.gov/bridge/nbi/ascii.cfm>
702 (October 15, 2016)
703 Goodnight, J. C., Kowalsky, M. J., and Nau, J. M. (2016). “Strain Limit States for Circular RC
704 Bridge Columns.” *Earthquake Spectra*, *32*(3), 1627–1652.
705 Haselton, C. B., and Deierlein, G. G. (2008). “Assessing Seismic Collapse Safety of Modern
706 Reinforced Concrete Moment-Frame Buildings.” *Report No. PEER 2007/08*, Pacific
707 Earthquake Engineering Research Center.
708 Jeon, J.-S., DesRoches, R., and Lee, D. H. (2016). “Post-Repair Effect of Column Jackets on
709 Aftershock Fragilities of Damaged RC Bridges Subjected to Successive Earthquakes.”
710 *Earthquake Engineering and Structural Dynamics*, *45*, 1149–1168.
711 Jeong, H. I., Sakai, J., and Mahin, S. A. (2008). "Shaking Table Tests and Numerical Investigation
712 of Self-Centering Reinforced Concrete Bridge Columns.” *Report No. PEER 2008/06*,

713 Pacific Earthquake Engineering Research Center.
714 Jiang, T., and Teng, J. G. (2007). “Analysis-Oriented Stress-Strain Models for FRP-Confined
715 Concrete.” *Engineering Structures*, *29*(11), 1698–3968.
716 Jung, D., Wilcoski, J., and Andrawes, B. (2018). “Bidirectional Shake Table Testing of RC
717 Columns Retrofitted and Repaired with Shape Memory Alloy Spirals.” *Engineering*
718 *Structures*, *160*, 171–185.
719 Kawashima, K., and Unjoh, S. (1997). “The Damage of Highway Bridges in the 1995 Hyogo-Ken
720 Nanbu Earthquake and Its Impact on Japanese Seismic Design.” *Journal of Earthquake*
721 *Engineering*, *1*(3), 505–541.
722 Ketchum, M., Chang, V., and Shantz, T. (2004). “Influence of Design Ground Motion Level on
723 Highway Bridge Costs.” *Report No. PEER 6D01*, Pacific Earthquake Engineering
724 Research Center.
725 Konstantinidis, D., Kelly, J. M., and Makris, N. (2008). “Experimental Investigation on the seismic
726 response of bridge bearings.” *EERC 2008-02*, Earthquake Engineering Research Center,
727 Univerisity of California.
728 Lee, W. K., and Billington, S. L. (2011). “Performance-Based Earthquake Engineering
729 Assessment of a Self-Centering, Post-Tensioned Concrete Bridge System.” *Earthquake*
730 *Engineering and Structural Dynamics*, *40*(8), 887–902.
731 Lehman, D. E., Gookin, S. E., Nacamuli, A. M., and Moehle, J. P. (2001). “Repair of Earthquake-
732 Damaged Bridge Columns.” *ACI Structural Journal*, *98*(2), 233–242.
733 Liel, A. B., Haselton, C. B., Deierlein, G. G., and Baker, J. W. (2009). “Incorporating Modeling
734 Uncertainties in the Assessment of Seismic Collapse Risk of Buildings.” *Structural Safety*,
735 *31*(2), 197–211.

736 Mackie, K. R., Wong, J.-M., and Stojadinovic, B. (2008). “Integrated Probabilistic Performance-
737 Based Evaluation of Benchmark Reinforced Concrete Bridges.” *Report No. PEER*
738 *2007/09*, Pacific Earthquake Engineering Research Center.
739 Mackie, K. R., Wong, J.-M., and Stojadinovic, B. (2011). “Bridge Damage and Loss Scenarios
740 Calibrated by Schematic Design and Cost Estimation of Repairs.” *Earthquake Spectra*,
741 *27*(4), 1127–1145.
742 Mander, J. B., Priestley, M. J. N., and Park, R. (1988). “Theoretical Stress-Strain Model for
743 Confined Concrete.” *Journal of Structural Engineering*, *114*(8), 1804–1826,
744 10.1061/(ASCE)0733-9445(1988)114:8(1804).
745 Mander, John B., Panthaki, F. D., and Kasalanati, A. (1994). “Low-Cycle Fatigue Behavior of
746 Reinforcing Steel.” *Journal of Materials in Civil Engineering*, *6*(4), 453–468,
747 10.1061/(ASCE)0899-1561(1994)6:4(453).
748 Mattock, A. H., Kriz, L. B., and Hognestad, E. (1961). “Rectangular Concrete Stress Distribution
749 in Ultimate Strength Design.” *Journal of American Concrete Institute*, *57*(2), 875–928.
750 McKenna, F., Fenves, G. L., and Scott, M. H. (2000). “Open System for Earthquake Engineering
751 (Version 2.2.2).” Pacific Earthquake Engineering Research Center, Berkeley, CA.
752 Padgett, J. E., & DesRoches, R. (2007). Sensitivity of Seismic Response and Fragility to Parameter
753 Uncertainty. *Journal of Structural Engineering*, *133*(12), 1710–1718.
754 https://doi.org/10.1061/(ASCE)0733-9445(2007)133:12(1710)
755 Padgett, J. E., and DesRoches, R. (2008). “Methodology for the Development of Analytical
756 Fragility Curves for Retrofitted Bridges.” *Earthquake Engineering and Structural*
757 *Dynamics*, *37*(8), 1157–1174.
758 Padgett, J. E., and DesRoches, R. (2009). “Retrofitted Bridge Fragility Analysis for Typical

759 Classes of Multispan Bridges." *Earthquake Spectra*, *25*(1), 117–141.
760 Priestley, M. J. N., Seible, F., Xiao, Y., and Verma, R. (1994). "Steel Jacket Retrofitting of
761 Reinforced Concrete Bridge Columns for Enhanced Shear Strength - Part 2: Test Results
762 and Comparison with Theory." *ACI Structural Journal*, *91*(5), 537–551.
763 Ryan, S. E., and Porth, L. S. (2007). "*A* Tutorial on the Piecewise Regression Approach Applied
764 to Bedload Transport Data." *Report No. RMRS-GTR-189*, Department of Agriculture,
765 Forest Service, Rocky Mountain Research Station.
766 Saini, A., and Saiidi, M. S. (2013). "Post-Earthquake Damage Repair of Various Reinforced
767 Concrete Bridge Components." *Report No. CA 13-2180,* Department of Civil and
768 Environmental Engineering, University of Nevada, Reno.
769 Spoelstra, M. R., and Monti, G. (1999). "FRP-Confined Concrete Model." *Journal of Composites*
770 *for Construction*, *3*(3), 143–150, 10.1061/(ASCE)1090-0268(1999)3:3(143).
771 Tapia, C., and Padgett, J. E. (2016). "Multi-Objective Optimization of Bridge Retrofit and Post-
772 Event Repair Selection to Enhance Sustainability." *Structure and Infrastructure*
773 *Engineering*, *12*(1), 93–107.
774 Tazarv, M., and Saiidi, M. S. (2013). "Analytical Studies of the Seismic Performance of a Full-
775 Scale SMA-Reinforced Bridge Column." *International Journal of Bridge Engineering*,
776 *1*(1), 37–50.
777 Tazarv, M., and Saiidi, M. S. (2015). "Reinforcing NiTi Superelastic SMA for Concrete
778 Structures." *Journal of Structural Engineering*, *141*(8), 10.1061/(ASCE)ST.1943-
779 541X.0001176, 04014197.
780 Vamvatsikos, D., and Cornell, C. A. (2002). "Incremental Dynamic Analysis." *Earthquake*
781 *Engineering and Structural Dynamics, 31*, 491–514.

782 Veletzos, M. J., Panagiotou, M., and Restrepo, J. I. (2006). “Post Seismic Inspection and Capacity
783 Assessment of Reinforced Concrete Bridges.” *Report No. SSRP-06/19*, University of
784 California, San Diego.
785 Vosooghi, A., and Saiidi, M. S. (2010). “Post-Earthquake Evaluation and Emergency Repair of
786 Damaged RC Bridge Columns Using CFRP Materials” *Report No. CCEER-10-05*, Center
787 for Civil Engineering Earthquake Research, University of Nevada, Reno.
788 Vosooghi, A., and Saiidi, M. S. (2013a). “Design Guidelines for Rapid Repair of Earthquake-
789 Damaged Circular RC Bridge Columns Using CFRP.” *Journal of Bridge Engineering*,
790 *18*(9), 827–836, 10.1061/(ASCE)BE.1943-5592.0000426
791 Vosooghi, A., and Saiidi, M. S. (2013b). “Shake-Table Studies of Repaired Reinforced Concrete
792 Bridge Columns Using Carbon Fiber-Reinforced Polymer Fabrics.” *ACI Structural*
793 *Journal*, *110*(1), 105–114.
794 Yang, C., DesRoches, R., and Padgett, J. (2009). “Fragility Curves for a Typical California Box
795 Girder Bridge.” *Proc., Technical Council on Lifeline Earthquake Engineering Conference*,
796 American Society of Civil Engineers, Oakland, California, 47-58.
797 Yang, Y., Sneed, L. H., Morgan, A., Saiidi, M. S., and Belarbi, A. (2015). “Repair of RC Bridge
798 Columns with Interlocking Spirals and Fractured Longitudinal Bars - An Experimental
799 Study.” *Construction and Building Materials*, *78*, 405–420.
800 Zerbe, R. O., and Falit-Baiamonte, A. (2001). “The Use of Benefit-Cost Analysis for Evaluation
801 of Performance-Based Earthquake Engineering Decisions” *Report No. PEER 2002/06*,
802 University of Washington: Pacific Earthquake Engineering Research Center.
803